Wind and Structures, Vol. 11, No. 2 (2008) 75-96
DOI: http://dx.doi.org/10.12989/was.2008.11.2.075

CFD simulations of the flow field of a laboratory-simulated tornado for parameter sensitivity studies and comparison with field measurements

Le Kuai*, Fred L. Haan, Jr.‡, William A. Gallus, Jr.‡† and Partha P. Sarkar‡‡

Iowa State University, Ames, IA 50011, USA
(Received June 27, 2007, Accepted February 15, 2008)

Abstract. A better understanding of tornado-induced wind loads is needed to improve the design of typical structures to resist these winds. An accurate understanding of the loads requires knowledge of near-ground tornado winds, but observations in this region are lacking. The first goal of this study was to verify how well a CFD model, when driven by far field radar observations and laboratory measurements, could capture the flow characteristics of both full scale and laboratory-simulated tornadoes. A second goal was to use the model to examine the sensitivity of the simulations to various parameters that might affect the laboratory simulator tornado. An understanding of near-ground winds in tornadoes will require coordinated efforts in both computational and physical simulation. The sensitivity of computational simulations of a tornado to geometric parameters and surface roughness within a domain based on the Iowa State University laboratory tornado simulator was investigated. In this study, CFD simulations of the flow field in a model domain that represents a laboratory tornado simulator were conducted using Doppler radar and laboratory velocity measurements as boundary conditions. The tornado was found to be sensitive to a variety of geometric parameters used in the numerical model. Increased surface roughness was found to reduce the tangential speed in the vortex near the ground and enlarge the core radius of the vortex. The core radius was a function of the swirl ratio while the peak tangential flow was a function of the magnitude of the total inflow velocity. The CFD simulations showed that it is possible to numerically simulate the surface winds of a tornado and control certain parameters of the laboratory simulator to influence the tornado characteristics of interest to engineers and match those of the field.

Keywords: tornado wind field; CFD simulation; laboratory tornado simulator; Doppler radar observation; tornado-like vortex; near-ground flow.

1. Introduction and objectives

Near-surface wind speeds in a tornado can exceed 100 m/s and cause significant damage, as the swirling winds exert greater loads on structures than straight-line winds (Jischke and Light 1983). Statistics show that 90% of tornadoes have F2 strength winds or weaker (Bluestein 1993). Given

* Graduate Research Assistant, Dept. of Geological and Atmospheric Sciences, E-mail: kuaile@iastate.edu
‡ Assistant Professor, Corresponding Author, Dept. of Aerospace Engineering, E-mail: haan@iastate.edu
‡† Professor, Dept. of Geological and Atmospheric Sciences, E-mail: wgallus@iastate.edu
‡‡ Professor/Wilson Chair, Dept. of Aerospace Engineering, E-mail: ppsarkar@iastate.edu

this fact, it may be possible to design low-rise structures such as residential buildings to withstand the large majority of tornado events. Only certain facilities, for example, power plants, hospitals and schools, would need to be designed for F3 or higher intensity tornadoes. Our primary goal involving numerical simulation of tornadoes is to learn more about the near-ground flow field in tornadoes to assist in determining tornado-induced wind loads on typical structures so that these structures might be better designed to withstand F0-F2 tornadoes.

This paper focuses on numerical simulation of tornado-like vortices and compares the simulated velocity data with both laboratory and field measurements. Numerical simulation was performed using FLUENT CFD software (Fluent 2005) while laboratory simulation was conducted with the Iowa State University (ISU) Tornado/Microburst Simulator. Field measurements were obtained from Doppler-on-Wheels (DOW) radar measurements of an F4 tornado that occurred at Spencer, South Dakota on May 30, 1998 (Wurman and Alexander 2005). The objectives of the work reported herein were:

(a) To build a numerical model representing the ISU laboratory tornado simulator to explore parameter sensitivity of tornado-like vortex simulations. The effect of parameters such as inflow depth, inflow radius, surface roughness, swirl ratio, outflow radius, location of outflow with respect to ground plane, mesh size and boundary conditions were studied.
(b) To use the numerical model to study the flow field in a tornado-like vortex generated with Doppler radar velocity data as input. The numerical model velocity data from elevations greater than 20 m (including cases with surface roughness) were used to evaluate the capability of the model to simulate the Doppler radar velocity field.
(c) To use the velocity data from laboratory measurements far from the center of the tornado as input for the numerical model to check how well the model reproduces the velocity distribution of the laboratory simulation.

An understanding of these sensitivities will assist in the design of later numerical or laboratory experiments exploring the near ground flow more closely. The work reported in this paper was reported in preliminary form in Gallus, *et al*. (2004 and 2006).

2. Background

2.1. Laboratory simulation

Some of the pioneering work to better understand tornado structure used physical models (such as Ward 1972) to simulate tornado-like vortices. A number of other tornado simulators were later designed and tested based on Ward's prototype (Doswell and Grazulis 1998). Other successful physical models were designed by Leslie (1977), Church, *et al.* (1979) and Snow and Lund (1988). Based on a physical model, Davies-Jones (1973), for instance, showed that a single concentrated vortex would form only for intermediate values of swirl ratio.

The final design of the ISU laboratory simulator is unique in comparison to previously constructed simulators in that it can translate a vortex by forcing it entirely from above in a manner that may replicate nature. Fig. 1(a) is a schematic depicting the structure and dimensions of the simulator when used to produce either a tornado or a microburst. A 1.83 m (6 ft)-diameter fan that can generate updraft flow rates of about 40 m^3/s is at the center of this simulator. Two concentric circular cylinders – 5.5 m (18 feet) and 4.9 m (16 feet) in diameter and 3.35 m (11 feet) in height – form a 0.3 m (1 ft) wide outer duct that surrounds the fan and is connected to it at the top through

two parallel circular disks 0.3 m (1 ft) apart. The entire simulator assembly is suspended from a 2250-kg (5 ton) capacity crane so that it can move along a track over a 10.4 m (34 ft) long by 6.1 m (20 ft) wide ground plane. The fan includes a flow-conditioning honeycomb and screen and produces an updraft at the center of the simulator. The upward flow through the fan comes out of the outer duct as a downdraft. Equally-spaced vanes along the periphery of the inner cylinder of the outer duct impart rotation to the downdraft flow. The vorticity present in the low-level inflow is stretched beneath the updraft fan forming a tornado that travels along the ground plane as the simulator translates. This design permits a maximum tornado diameter of 1.12 m (3.7 ft.), i.e., the distance between the maximum tangential speeds. Swirl ratio (*S*) is the ratio of the vortex

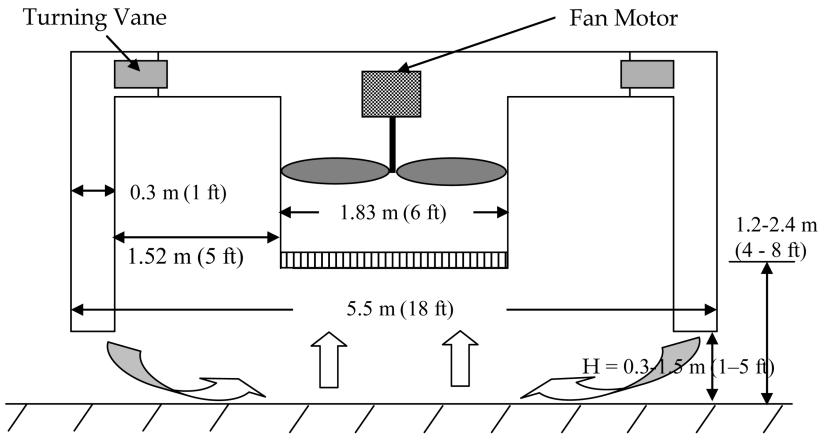

(a)

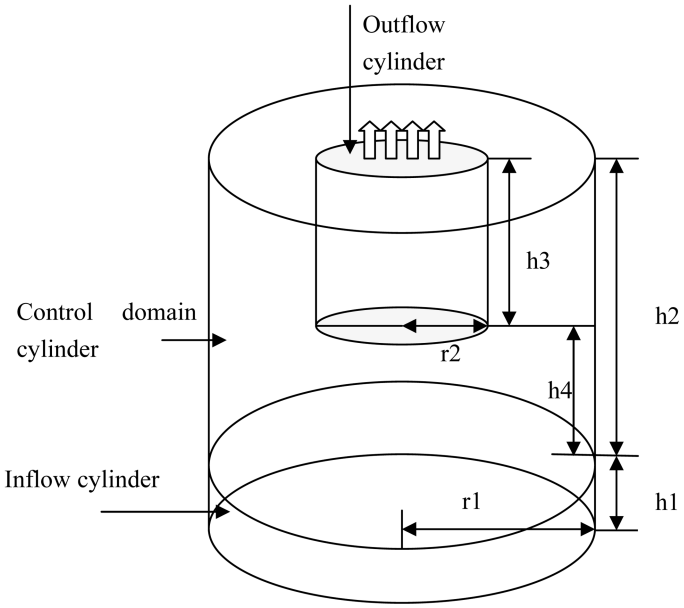

(b)

Fig. 1 (a) Schematic diagram illustrating the principle of operation of the tornado simulator. (b) Geometric parameters of the numerical model

circulation to the accompanying inflow rate. The maximum S measured in the ISU Laboratory Tornado Simulator was 1.14. This swirl ratio is based on the following modified definition, $S = \pi r_c^2 V_t / Q$ where V_t is the maximum tangential speed, r_c, is the radius at which V_t occurs and Q is the total inflow rate. While swirl ratios have in the past often been calculated with updraft radius rather than core radius, updraft radius is not at all easily discernible from a single-radar data set while core radius is. For this reason, this modified swirl ratio was used. This value will typically be less than swirl ratios computed using the conventional formulation where circulation is calculated at the maximum radius of the updraft (for a Rankine vortex, the current swirl ratio would be less than conventional values by a factor of r_c/r_u where r_u is the radius of the updraft). The peak translation speed of the vortex is 0.61 m/s (2 ft/sec). The vortex height can vary from 1.22 to 2.44 m (4 to 8 ft) by adjusting the ground plane up or down. Models of structures with geometric scales of 1/100 to 1/500 can be placed in the path of the vortex for measurement of surface pressures or overall loads acting on them.

2.2. Numerical simulation

More recently, numerical simulation has replaced the laboratory simulator as the primary tool to study tornado vortex dynamics due to reduced costs and increased versatility. Some pertinent results inferred from numerical simulations follow. Diamond and Wilkins (1984) found that surface roughness might intensify a translating vortex but decrease the swirl ratio of a stationary vortex. Considering turbulence in determining the interaction with the surface, Lewellen, D.C. and Lewellen, W.S. (1997) addressed the sensitivity of vortex structure to swirl ratio and to translation speed by examining a large eddy simulation (LES) of turbulent transport in a tornado. They found that the structure of the turbulent central vortex corner flow could be strongly affected by some physical parameters, such as surface roughness, tornado translation speed, and near ground inflow distribution, even under the same large-scale swirl ratio. Lewellen, *et al*. (1999) studied the influence of local swirl ratio and interaction of the surface roughness on the tornado corner region. They found that the local swirl ratio can be reduced (increased) by anything that increases the low level inflow (upper-core radius). The above studies highlight the importance of the interaction between the surface roughness and the tornado. An increase in surface roughness leads to lower swirl flow-like behavior. It has also been suggested that the maximum velocities occur quite close to the surface (Lewellen, *et al*. 1999, Lewellen, D.C. and Lewellen, W.S. 2007a, 2007b), a result with significant consequences for engineered structures.

2.3. Field measurement

In recent years, portable Doppler radars have been successfully deployed in close proximity to tornadoes providing a detailed picture of wind flow in and near tornadoes (Bluestein and Pazmany 2000, Wurman and Gill 2000, Wurman 2002, Alexander and Wurman 2005). However, because of the beam angle required to prevent interference from ground-based obstacles and the finite resolution of the data, radar measurements do not extend below 20-50 m above the ground. Although one goal of the VORTEX-II experiment proposed for 2009 (P. Markowski, Pennsylvania State University, 2007, personal communication) is to obtain measurements of wind in the lowest 20-50 m of a tornado through deployment of new technologies, until that time the best estimates of near-ground flow may require the use of numerical models.

3. Experimental measurements

3.1. Doppler radar observations

On the evening of 30 May 1998, at least two strong tornadoes occurred across South Dakota causing significant (F4) property damage and 6 deaths (Alexander and Wurman 2005). The primary observational radar data used in our numerical simulations came from the second violent tornado as it passed through Spencer at 0134 UTC (8:34 pm CDT) observed by the DOW mobile radars recording two- and three-dimensional wind fields. The tornado center was closest in its approach of DOW-3 at about 0134 UTC (Alexander and Wurman 2005). The core radius of the second tornado increased from 125 m early in its life to 200 m by 0141 UTC and then decreased in size slowly. However, tornado damage was found to occur not only within the core radius but also over a broader area (Wurman and Alexander 2005).

Figures 2 and 3 show the instantaneous tangential and radial speed profiles in the Spencer, South Dakota tornado as measured by DOW velocity observations. The original data were fitted into an axisymmetric model constrained by the radar data to eliminate some higher wave-number perturbations such as multiple vortices. This model incorporates the tornado wind field components of axisymmetric rotation and translation. The model domain covered a 2 km by 2 km area with 20 m horizontal grid spacing. The radar-scan time for each elevation was around 5 seconds. A least squares minimization of the Doppler velocity observations was applied to estimate the azimuthally averaged (axisymmetric) radial and tangential wind speed components in 40 m wide annuli at successive 20 m intervals moving out from the tornado center. These estimates are tornado-relative and do not include the translation speed. To obtain the stationary, axisymmetric rotation speed, the translational motion was subtracted from the observed wind speed.

The radar data analyzed contain the tangential speeds from 20 m to 660 m above ground and radial speeds within 1000 m from the center of the tornado. The tangential speed (Fig. 2) along a radius has one peak value, the core radius, which increases with height from 120m to 250 m so that the tornado vortex has a funnel shape. The broadening is concentrated in the 50-80 m layer. Maximum tangential speeds decrease from low levels to higher levels with the 20 m and 50 m values 20% larger than speeds at higher elevations.

Radial speed profiles as a function of height at different distances from the center of the tornado are shown in Fig. 3. Negative values represent inflow. At 1000 m radius, inflow occurs at all levels below 400 m, but the depth of the inflow layer gradually decreases closer to the center of the vortex. The maximum radial speed is located at 20 m above ground, which is the lowest level for which data are available. Numerical simulations (e.g. Lewellen, *et al.* 1999, Bluestein and Pazmany 2000) indicate that strongest inflow may occur potentially only 10-20 m above ground.

Radar data at 0134:23 UTC were chosen as the inflow conditions for our numerical simulations because the vortex was closest to the radar at this time, allowing data to be obtained closest to the ground (at 20 m). It should be noted, however, that radar data in three other volume sets spaced one minute apart after 0134:23 UTC were also analyzed, and it was found that the tornado wind distribution changed rapidly. Most of the variations in velocities found in the sensitivity tests to follow are smaller than the changes observed to occur in the tornado within time periods of only a minute or two. In the comparisons of numerical simulation results to radar observations that were performed in this paper, it should be noted that the radar data used in the axisymmetric model were acquired over a finite length of time. Thus, the radar observations presented here have essentially

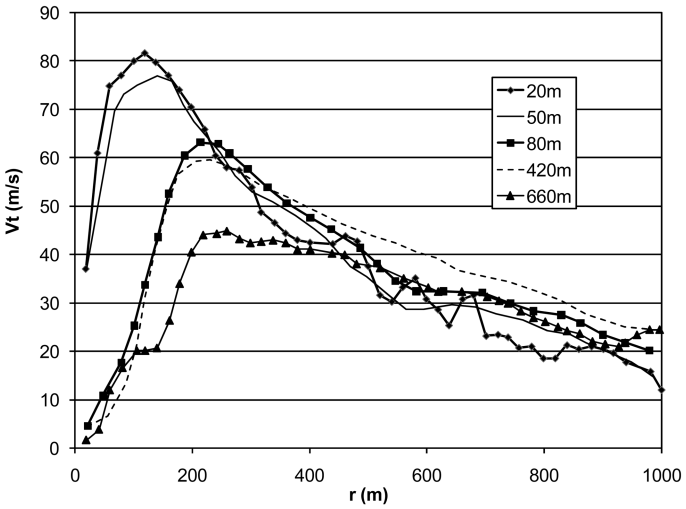

Fig. 2 Radar-observed tangential speed profiles (m/s) as a function of radial distance (m). Different curves show profiles at different elevations (m) above ground

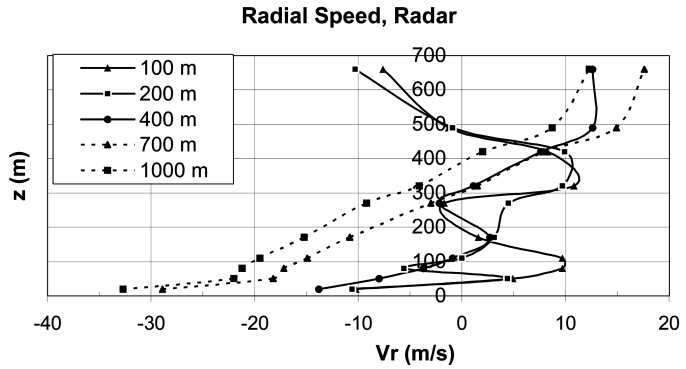

Fig. 3 Radar-observed radial speed profiles (m/s) averaged azimuthally as a function of height (m). Different curves refer to different radial distances (m) from the center of the vortex

been time averaged, and calculated on the basis of an axisymmetric vortex. The numerical simulations that yield a steady-state velocity structure within the vortex are based on fixed boundary and initial conditions, as specified by the user, but the tornado in nature is subject to unsteady boundary conditions which could be one of the reasons that a violent tornado is a rare event (Lewellen, *et al.* 1999). Because of this discrepancy, the numerical simulations cannot be expected to match the radar observations exactly. The primary emphasis of this study was to determine the sensitivity to changes in model parameters rather than to identify the specific configuration that exactly duplicates radar observations, although parameters that help to do so are of interest for future laboratory simulations.

3.2. Laboratory measurement

Velocity fields in the ISU Tornado/Microburst Simulator were measured using a spherical 18-hole

pressure probe (PS18 Omniprobe from Dantec). The pressures from the probe were measured with a Scanivalve ZOC33/64 Px electronic pressure scanner. The 18-hole probe is conceptually organized to form a network of five-hole configurations (some ports/holes are shared by two groups) so that it can measure flow angularity up to 165 degrees with respect to the probe axis. The calibration software supplied with the probe uses a local least squares fit with this network of 5-hole configurations to provide accuracy of 2% for velocity magnitude and 1.5 degrees for velocity angle.

Velocities were measured at two levels from the ground plane, z = 5.08cm (2 in.) and 34.3cm (13.5 in.). For each measurement, the ground plane was fixed at 45.7cm (18 in.) below the exit of the outer duct, the vane angles were set to 55 degrees and the fan speed was fixed at one third of full speed (at this speed, flow rate was 15.9 m^3/sec at zero vane angle and 7.6 m^3/sec at 55-degree vane angle). The measurements were made with a stationary tornado. The core radius and the peak tangential speed at 12.7cm height were measured as 0.53 m and 9.7 m/s, respectively, and at 5.08 cm height were measured as 0.38 m and 11.8 m/s, respectively. Swirl ratio, S, was estimated to be 1.14 for the 55-degree vane angle setting.

4. Description of numerical model

The geometric model used here, resembling the ISU laboratory simulator, consists of three cylinders, an inflow cylinder at the bottom, an outflow cylinder at the top and a control domain cylinder outside the outflow cylinder (Fig. 1b). In order to generate an axisymmetric vortex, axisymmetric boundary conditions were applied to the domain with initially sheared inflow entering the bottom cylindrical domain with radial and tangential speed components. Flow exits the big cylinder only through the small central cylinder at the top boundary. The radius of the bottom cylinder (r1) represents the inflow radius where the initial inflow condition is defined. The radius of the top outflow cylinder (r2) could be thought to represent the radius of the thunderstorm updraft.

In the design of the CFD domain, one important consideration was the size of r1. Additionally, an appropriate mesh size had to be determined – one that was small enough to accurately depict wind variations within the tornado close to the ground but large enough to allow the simulation to run with limited computational resources. Since the primary concern was the surface-layer wind profile, the mesh size at near-ground levels was chosen to be finer than at higher levels. Although radar data were provided to an elevation of 660 m, no observational information was available to indicate the height of the cloud base, which in nature would represent a level above which strong ascent is occurring due in large part to buoyancy forces. In our simulations, buoyant effects are not directly included, although the inflow velocities provided by radar observations reflect the storm-scale circulation for the Spencer tornado case which was driven largely by buoyant forces. The neglect of buoyancy in the numerical simulations may impact the simulations somewhat, but problems should be minimized by the use of observed inflow profiles. The impact of surface roughness was investigated by putting rings of finite height on the ground in the model domain.

A fine grid for this geometry was generated using the software package Gambit, and FLUENT was used to find steady-state solutions to the 3D Navier Stokes equations and the RNG k-ε model. The k-ε model is used frequently in engineering studies to simulate boundary layer evolution, flow over changes in roughness and topography, and sea-breeze fronts (Stull 1988). It has been applied also for studying tornado-structure interaction and resulting structural loading (Selvam and Millett 2003).The Navier Stokes equations included the mass and momentum conservation equations as

given by:

$$\frac{\partial \rho}{\partial t} + \nabla \cdot (\rho \vec{u}) = 0 \tag{1}$$

$$\frac{\partial}{\partial t}(\rho \vec{u}) + \nabla \cdot (\rho \vec{u} \vec{u}) = -\nabla p + \nabla \cdot (\bar{\bar{\tau}}) \tag{2}$$

where the viscous stress tensor $\bar{\bar{\tau}}$ is given as:

$$\bar{\bar{\tau}} = \mu \left[(\nabla \bar{u} + \nabla \bar{u}^T) - \frac{2}{3} \nabla \cdot \bar{u} I \right] \tag{3}$$

The RNG k-ε model then includes the following two equations for turbulent kinetic energy, k, and dissipation rate, ε:

$$\frac{\partial}{\partial t}(\rho k) + \nabla \cdot (\rho k \vec{u}) = \nabla \cdot [\alpha_k \mu_{eff} \nabla k] - \rho \overline{u_i' u_j'} \frac{\partial u_j}{\partial x_i} - \rho \varepsilon \tag{4}$$

$$\frac{\partial}{\partial t}(\rho \varepsilon) + \nabla \cdot (\rho \varepsilon \vec{u}) = \nabla \cdot [\alpha_\varepsilon \mu_{eff} \nabla \varepsilon] - \rho C_{1\varepsilon} \frac{k}{\varepsilon} \rho \overline{u_i' u_j'} \frac{\partial u_j}{\partial x_i} - \rho C_{2\varepsilon} \frac{\varepsilon^2}{k} + \frac{C_\mu \rho \eta^3 (1 - \eta/\eta_0)}{1 + \beta \eta^3} \frac{\varepsilon^2}{k} \tag{5}$$

where $C_{1\varepsilon} = 1.42$, $C_{2\varepsilon} = 1.68$, $\eta_0 = 4.38$, $\eta = Sk/\varepsilon$ and $S = \sqrt{2 S_{ij} S_{ij}}$ (in this equation, S is the modulus of the rate-of-strain tensor). The inverse effective Prandtl numbers, α_k and α_ε, in the high Reynolds number limit are $\alpha_k = \alpha_\varepsilon = 1.393$. Effective viscosity is computed from $\mu_{eff} = \rho C_\mu k^2/\varepsilon$ with $C_\mu = 0.09$. More details of the implementation of the model can be found in the FLUENT documentation (2005).

Both Hex/Wedge and Tet/Hybrid mesh elements were used to mesh the domain. The inlet vertical speed was assumed to be zero, while at the outlet boundary the radial and tangential components were assumed to be zero. All other boundaries were defined to be solid walls with no-slip boundary conditions. Standard wall functions were applied to resolve the flow near the walls. The standard wall functions work quite well for a broad range of wall-bounded flows.

Boundary conditions for the domain were specified as follows. Through the h1 cylinder, the velocity profiles were specified to match the Spencer tornado by radial, tangential and vertical components, i.e.:

$$\begin{aligned} u_r(r = r_1,\ 0 \le z \le h_1) &= u_r\big|_{Spencer} \\ u_\theta(r = r_1,\ 0 \le z \le h_1) &= u_\theta\big|_{Spencer} \\ u_z(r = r_1,\ 0 \le z \le h_1) &= u_z\big|_{Spencer} \end{aligned} \tag{6}$$

The boundary conditions for the floor, h2 cylinder, h3 cylinder and the annula at the roof were set as viscous walls (i.e. no slip).

In all simulations except the ones considering the effect of surface roughness, a smooth ground plane was assumed. Therefore, vortex parameters such as angular velocity, decay rate of the tangential speeds outside the core region, core radius and the magnitude of the peak tangential speed were not expected to match those observed by radar, since it is known that surface roughness affects these values. The smooth ground plane cases were used for studying the sensitivity effects of

parameters other than surface roughness. For cases where surface roughness was included in the numerical model, a comparison of numerical results and field observations was considered a reasonable match if the vortex parameters listed above compared well at lower levels. Our comparisons of numerical simulation results with field data were made at 110 m AGL because field roughness did not appear to significantly affect vortex parameters at that level; the Spencer tornado vortex was found to increase in size from 20 m to 80 m but remained relatively constant in size and velocity above 80 m. Additional mismatch between the numerical and observational data might occur because of measurement uncertainties in the Doppler data, such as differences between air motion and debris motion (Dowell, *et al*. 2005). Doppler radars sample the motion of objects within the tornado instead of the actual airflow and these objects move tangentially more slowly than and outward relative to the air, so that the Doppler data likely underestimate the real wind speeds (Dowell, *et al*. 2005).

A geometric length scale based on the inflow radius was chosen for comparison of laboratory simulator dimensions with those of the numerical model and full-scale observations. Comparing an inflow radius of 800 m in the full scale dataset with an inflow radius or inside radius of 2.44 m (96 in.) in the laboratory simulator's outer duct yields a geometric scale of approximately 330. Thus, field data available at the 110m height in full scale can be compared with those measured at 34cm (13.5 in.) height in the laboratory. The radius of the duct that houses the laboratory simulator fan (0.91 m or 3 ft) scales up as the outflow radius of the numerical model (r2) to be about 300 m. The length of the numerical model control domain cylinder (h2) compares with the total height of the outer laboratory cylinder (3.35 m or 11 ft) and scales to ~1100 m; and the length of the numerical model outflow cylinder (h3) compares with the total length of the fan duct and the space above it (1.52 m or 5 ft) in the lab simulator and scales to ~500 m. These scaled values were used for Case 1 listed in Table 1; Cases 2-19 are variations of this case to study the sensitivity of results to each parameter.

5. Results—parameter sensitivity tests

The results of the sensitivity analysis for the following geometric parameters of the numerical domain are presented in Tables 2 and 3 and are discussed in the following sections.

5.1. Mesh size

Mesh size is an important factor likely affecting all output parameters of the numerical model. Although grid independence is a desirable objective in simulations of meteorological events that have a large grid domain, it is almost impossible to achieve it because of limited computational resources. Grid sizes of 10-20 km are now used operationally (http://www.ncep.noaa.gov) to simulate thunderstorm systems, and some of the best research simulations use spacings as fine as 1-2 km (see Wicker and Wilhelmson 2001, for a review). Only a very few simulations have been done with spacings as fine as 100 m or 50 m within small nested domains (Hu, *et al*. 2004). Since one of the main objectives of this study was to simulate wind close to the ground, a finer grid than those used earlier by others was deemed necessary.

To examine how fine a grid is needed to accomplish convergence to acceptable results, the effect of grid size on the output parameters was studied systematically (Table 1, Fig. 4) using grid sizes (both horizontal and vertical) of 40, 20, 10, and 5 m up to a height of 70 m while keeping all other

Table 1 Parameters of the numerical domain for case studies

Case	Test Parameter	Surface Roughness	Outflow Radius r2 (m)	Inflow Radius r1 (m)	Mesh Type	Inflow Depth h1 (m)	Length of Control Domain Cylinder h2 (m)	Length of Outflow Cylinder h3 (m)	Note
Doppler Radar Velocity Input at 800 m or 1000 m from the Vortex Center									
Case 1	Original Case	Smooth	300	800	2	270	1100	500	BC1, VD1
Case 2	Inflow Radius		300	1000	2	400	1100	500	BC1, VD2
Case 3	Outflow Radius		350	800	2	270	1100	500	BC1, VD1
Case 4			375	1000	2	400	1100	500	BC1, VD2
Case 5	Length of Control Domain		300	800	2	270	800	500	BC1, VD1
Case 6			300	800	2	270	1400	500	BC1, VD1
Case 7	Boundary Conditions		300	800	2	270	1100	500	BC2, VD1
Case 8	Surface Roughness	Rough 1	300	800	2	270	1100	500	BC1, VD1
Case 9		Rough 2	300	800	2	270	1100	500	
Case 10		Rough 3	300	800	2	270	1100	500	
Case 11	Swirl Ratio	Smooth	700	1000	2	400	1631	1137	VD2
Case 12			700	1000	2	400	1631	1137	VD3
Case 13			700	1000	2	400	1631	1137	VD4
Case 14			700	1000	2	400	1631	1137	VD5
Case 15			700	1000	2	400	1631	1137	VD6
Case 16			700	1000	2	400	1631	1137	VD7
Case 17			700	1000	2	400	1631	1137	VD8
Laboratory Velocity Input at 767 m (91.5 in. in laboratory scale) from the Vortex Center									
Case 18	Input	Smooth	300	800	2	134	800	500	BC1, VL
Case 19		Rough 4	300	800	2	134	800	500	

NOTES:
Scale: 1: 330, Laboratory Simulator versus Spencer 1998 Tornado based on R_c at 80-400 m;
Mesh 2: 5 m horizontal and vertical grid size up to 70 m height and 50 m grid above it;
BC1: Top Outflow Boundary Condition; BC2: Top and Side Outflow Boundary Condition;
Rough 1: Three rectangular rings 3 m high and 10 m wide at 200 m spacing starting at r = 200 m;
Rough 2: Three rectangular rings 5 m high and 10 m wide at 200 m spacing starting at r = 200 m;
Rough 3: Seven rectangular rings 5 m high and 10 m wide at 100 m spacing starting at r = 100 m;
Rough 4: Three rectangular rings 1 m high and 10 m wide at 200 m spacing starting at r = 200 m.
VD1: radial and tangential speeds at 800 m radius from observed radar data up to 270 m elevation with BC1; VD2: radial and tangential speeds at 1000 m radius from observed radar data up to 400 m elevation with BC1; VD3: VD2 except doubled radial speed; VD4: VD2 except halved radial speed; VD5: VD2 except doubled tangential speed; VD6: VD2 except halved tangential speed; VD7: VD2 with doubled radial and tangential speeds; VD8: VD2 with halved radial and tangential speeds; VL: radial and tangential speeds at 800 m radius from laboratory data up to 113 m elevation.

parameters at their Case 1 values. Additional cases were simulated with a 2.5 m mesh up to a 35 m height, and with a 10 m mesh up to a 140 m height. Above these lower elevations in all cases, a constant 50 m mesh was used. A larger mesh size was found to increase the core radius and decrease the peak tangential speed at the 20 m level (Table 2). The 20 m data do seem to converge as the mesh size is refined close to the ground. The lack of sensitivity at the 110 m level is likely because the mesh size remained unchanged above 35 m or 70 m for Meshes 1 to 5. A comparison of results for Mesh 6 and Mesh 3 shows that a finer mesh above 70 m elevation influences the core radius by 17% and peak tangential speed by 18% at the 110 m level and core radius by 8.4% with no change to tangential speed at the 20 m level. It is clear that a finer mesh (e.g., 2 m) would be desirable up to the elevation of interest to wind engineers (~500 m), but such a fine mesh was not

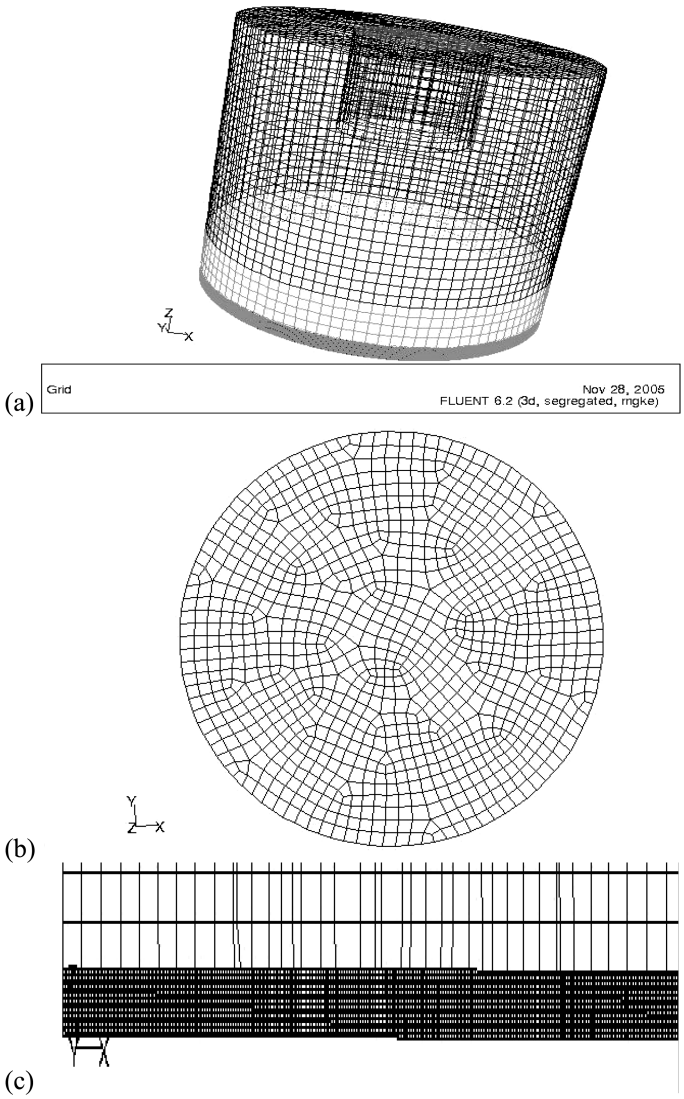

Fig. 4 Different views of Mesh 2 used in the numerical model. (a) 3-dimensional, (b) horizontal sweep surface, and (c) vertical sweep slice surface, with H=170 m

possible with the computer resources available to the authors. Based on the mesh convergence tests, the results obtained with Mesh 2, the primary one used in our study, seem to be within 20-30% of the converged values and were deemed acceptable for the sensitivity studies performed.

5.2. Inflow radius

Although the DOW radar dataset provided some information about the flow near the tornado at relatively low levels, the dataset was incomplete and some assumptions had to be made in the design of the numerical study. One of these assumptions concerned the distance away from the center of the tornado where the radar data would work best as prescribed inflow. Data were available outward to a distance of 1000 meters from the center of the tornado. The advantage of taking the 1000 m data to represent inflow into the idealized numerical model domain would be that this distance would be farthest from the tornado itself, and the model would have the greatest freedom to simulate a tornado with minimal influence from the boundary conditions. However, the farther the inflow is from the vortex core, the greater the influence of the ground roughness on the flow simulation. Since it is relatively difficult to model the terrain roughness in FLUENT, there is an advantage to using radar observations as inflow for the numerical model as close to the tornado as possible. However, in that case the boundary conditions might influence the simulation adversely.

Based on the above issues, sensitivity tests were performed using radar data at 800 m (Case 1) and 1000 m (Case 2) away from the tornado center as the inflow conditions prescribed on the outer cylinder of the numerical domain. As mentioned earlier, 800 m was chosen as the inflow radius for Case 1 because it represents the scaled up size of the 2.44 m (96 inch) radius of the outer duct in the lab model. This range of values selected for inflow radius is significantly greater than the maximum core radius (around 250 m) of the tornado vortex found in the field observations. Only negative radial speeds (toward the core) of the field observations were used along with the corresponding tangential speeds as input for the numerical model at 800 m and 1000 m radii. Thus, inflow depths (h1) of 270 m and 400 m at 800 m and 1000 m, respectively, were used.

Table 2 Results showing influence of mesh size

Mesh Type	Mesh Parameters			Core Radius r_c (m)		Maximum Tangential speed V_t (r_c) (m/s)	
	Cells	Nodes	Runtime (hrs)	Z = 20 m	110 m	20 m	110 m
Mesh 1	4,432,686	4,798,623	>10	63	107	190	124
Mesh 2	1,160,362	1,260,795	>7	68	107	176	122
Mesh 3	164,780	197,563	>5	83	107	164	127
Mesh 4	38,849	52,877	>2	95	107	124	123
Mesh 5	25,404	33,657	>0.5	105	107	69	121
Mesh 6	306,020	340,892	>6	90	89	165	150

Mesh 1: Case 1 from Table 1 but with 2.5 m horizontal and vertical grid up to 35 m height and 50 m grid above it.
Mesh 2: As in Mesh 1 but with 5 m grid up to 70 m height and 50 m grid above it.
Mesh 3: As in Mesh 1 but with 10 m grid up to 70 m height and 50 m grid above it.
Mesh 4: As in Mesh 1 but with 20 m grid up to 70 m elevation and 50 m grid above it.
Mesh 5: As in Mesh 1 but with 40 m grid up to 70 m elevation and 50 m grid above it.
Mesh 6: As in Mesh 1 but with 10 m grid up to 140 m height and 50 m grid above it.

Table 3 Numerical simulation results

Case Type	Swirl Ratio S	Core Radius r_c (m)		Maximum Tangential Speed V_t (r_c) (m/s)		Angular Velocity of the Core Ω (s^{-1})		Decay Rate n $V_t r^n = C$	
Z =		20 m	110 m	20 m	110 m	20 m	110 m	20 m	110 m
Radar Data	0.19	120	200	81	65	0.40	0.32	0.85	0.72
Case 1	0.17	68	107	176	122	2.24	0.48	0.95	0.76
Case 2	0.11	78	131	141	90	1.96	0.34	0.99	0.70
Case 3	0.15	74	107	157	111	2.15	0.51	0.93	0.69
Case 4	0.11	72	131	141	88	2.12	0.34	0.98	0.69
Case 5	0.18	70	107	192	130	2.50	0.53	0.99	0.79
Case 6	0.30	123	174	177	120	1.49	0.58	1.20	0.95
Case 7	0.19	148	174	125	87	0.77	0.42	1.16	0.75
Case 8	0.17	81	107	159	123	2.10	0.68	0.95	0.76
Case 9	0.21	181	213	74	63	0.40	0.27	0.97	0.69
Case 10	0.20	182	213	71	61	0.37	0.26	0.95	0.55
Case 11	0.09	118	137	90	66	1.02	0.53	0.98	0.63
Case 12	0.02	81	88	96	86	1.19	0.51	0.91	0.67
Case 13	0.44	190	257	58	46	0.22	0.20	0.98	0.65
Case 14	0.36	190	230	118	93	0.47	0.44	1.01	0.63
Case 15	0.02	75	88	61	44	0.84	0.32	0.93	0.66
Case 16	0.09	118	137	179	133	2.06	1.06	0.96	0.63
Case 17	0.09	118	137	45	33	0.59	0.27	0.98	0.63
Case 18	1.11	118	174	73	56	0.49	0.30	0.96	0.82
Case 19	1.65	134	214	70	56	0.40	0.27	1.00	0.93
Lab Data	1.14	125	184	79	65	0.69	0.49	1.25	0.94

Maximum tangential speeds were found to be greater and the core radius smaller as the inflow radius was reduced (compare Case 1 to Case 2 in Table 3). A larger inflow radius may allow a wider vortex. The difference in S between the two cases is mainly because of the difference in the flow rates (Q_{case1}/Q_{case2} =0.60).

5.3. Outflow radius

The radius of the outflow cylinder ($r2$) was varied from 300 m (Case 1) to 350 m (Case 3) and from 300 m (Case 2) to 375 m (Case 4) while all other parameters remained the same. An increase of the outflow radius was not found to change the core radius or the tangential speeds at all levels (Table 3). A comparison of core radii between Cases 4 and 1, however, where the ratio of the outflow radius to the inflow radius was the same (2.67), shows that an increase in the outflow radius can increase the core radius, resulting in a larger vortex.

5.4. Length of the control domain cylinder

In an additional test of sensitivity to the arbitrary amount of space within the control cylinder domain (h4), the length of the control domain cylinder (h2 in Fig. 1b) was varied while keeping h3, the length of the outflow cylinder, constant. The length of the control domain cylinder was reduced by 300 m from 1100 m (Case 1, h4 = 600 m) to 800 m (Case 5, h4 = 300 m) and increased by 300 m from 1100 m to 1400 m (Case 6, h4 = 900 m). Comparing Cases 5 and 1, the maximum peak tangential speed increased from 176 m/s to 192 m/s at 20 m above ground and increased slightly from 122 m/s to 130 m/s at 110 m above ground while core radii at both elevations did not change. The opposite was true for Case 6 versus Case 1 where peak tangential speeds remained almost the same while core radii at both elevations increased considerably. The h4/d2 ratio (where d2 is the diameter of the outflow cylinder) is equal to 1, 0.5, and 1.5 for Cases 1, 5, and 6, respectively, so one might conclude that beyond a critical h4/d2 of 1, as in Case 6, the tangential speeds do not change but core radius will increase. In contrast, below this critical value, as in Case 5, the tangential speeds will increase but the core radius will remain unchanged.

5.5. Boundary conditions

In all of the above cases, an outflow boundary condition was specified at the top of the outflow cylinder only (referred to as BC1 in Table 1) and the outflow was constrained elsewhere. In Case 7, an outflow boundary condition was added to the control cylinder allowing the flow to exit through its side surface as well (BC2, Table 1), a scenario better resembling natural tornadic storms. The resulting vortex was weaker and wider than in Case 1, and core radii and peak tangential speeds were much closer to those of the radar data. Some differences remained, which is understandable since the model was run with a smooth lower surface.

5.6. Surface roughness

In order to consider the effect of surface roughness in our simulations, three 10 m wide rings were used at radii of 600, 400 and 200 m with heights of 3 m (Rough 2, Case 8) and 5 m (Rough 2, Case 9). In Case 10, seven rings were built at every 100 m in the radial direction (Rough 3) in order to generate a greater surface roughness. This choice of surface roughness geometry (i.e., a few rings instead of numerous blocks) was an arbitrary trade off between grid generation and computational requirements. Large objects had to be placed near the ground to generate the large roughness values present in the real world. The aerodynamic roughness length is defined to be the height where the wind velocity decreases to zero. Many experiments have been done to study the relationship between roughness elements and the roughness length (Lettau 1969, Kondo and Yamazawa 1986) for boundary layer wind tunnel simulation of straight-line wind. However, these studies would not apply to the present case of tornado simulation where the available fetch over which the boundary layer develops is much smaller (1.8 m in lab scale) compared to a typical 15-20 m fetch in regular wind tunnels.

Increased roughness in Cases 8-10 (Table 3) was found to greatly reduce the tangential speed in a narrow layer close to the ground. With 3 m high roughness elements (Rough 1) in Case 8, the peak tangential speed at 20 m elevation was reduced by 10% from that of Case 1, but was still much stronger than the observed value. With 5 m roughness elements (Rough 2) in Case 9, the peak

tangential speed at 20 m was reduced by over half, and dropped to within 10% of the radar observations. Increased surface roughness also increased core radius and *S*. Assuming conservation of angular momentum, an enlarged core radius must be accompanied by reduced tangential speeds. Whereas Rough 1 did not produce any changes in the velocity or radius parameters at higher elevations such as 110 m compared to the smooth case, the larger roughness in Rough 2 did. The insignificant differences between Cases 9 and 10 suggest that the influence of roughness height is more pronounced (Case 9) than the roughness spacing (Case 10). The FLUENT simulations of the Spencer tornado agree with earlier studies (e.g. Dessens 1972) showing surface roughness to decrease peak tangential speeds at low levels and slightly increase the core radius.

5.7. Comparison of CFD simulation of lab data with lab measurement and radar data

Since the lab simulation is at a small scale, comparisons with radar observations and the numerical simulations driven by radar data require an upward scaling to the lab dimensions and velocities. As discussed earlier, a geometric scale of 1:330 was used between the laboratory and full scale. A velocity scale of 1:6.7 was obtained by comparing the peak tangential speed of the laboratory data and the radar data at 110 m elevation. Thereafter, the velocities at a 2.32 m (91.5 in.) radius in the laboratory scale and 767 m in the full scale were scaled up by the velocity scale and used as inflow in the numerical simulation of Cases 18 (smooth floor) and 19 (rough floor). Three rings of 1 m height and 10 m width were used at radii of 600, 400 and 200 m in Case 19 to simulate roughness. This roughness (Rough 4) was less pronounced than the roughness discussed in earlier tests (Rough 1-3). Fig. 5 shows that the numerical simulation results matched well with the lab profiles at an elevation of 110 m, especially in Case 18 as this lab simulation was performed above a smooth floor. The match becomes better when one uses the core radius for the length scale rather than the inflow radius (for velocity profiles scaled with the core radius, see Haan, *et al.* 2008). In these simulations, the inflow radius was used because it could be imposed in the CFD simulations while the core radius could not. This approach tested how well the computational simulation would reproduce the basic tornado structure. It did well. Case 19 matched the observed radar data slightly better than Case 18, likely because roughness does influence tornadoes in the field.

5.8. Swirl ratio

While previous cases examined computational domain geometric parameters, Cases 11-17 (Table 1) examined the effect of *S* on the tornado vortex by varying the inflow velocity (results shown in Table 3). The inflow radial and tangential speeds of Case 11 (VD2, Table 1) were varied while keeping the inflow depth unchanged. When the inflow rate (Q) was doubled by using doubled inflow radial speeds while keeping the inflow tangential speed unchanged (Case 12), *S* and tornado core radius decreased while the maximum tangential speed increased compared to Case 11. An increase in radial speed is equivalent to a decrease in the inflow angle with respect to the radius which is analogous to decreasing the laboratory simulator's vane angle. These results were consistent with observations of the impact of decreasing vane angle in the laboratory simulator. When the inflow rate (Q) was halved by using half of the inflow radial speed while keeping the inflow tangential speed unchanged (Case 13), *S* and tornado core radius increased while the maximum tangential speeds decreased compared to Case 11. A decrease in radial speed is

equivalent to an increase in the inflow angle. Once again the increase in S was consistent with laboratory observations. Cases 12 and 13 show that the core radius can be directly linked to S, i.e., larger S results in a larger vortex.

When the tangential speed was doubled (Case 14) from the control case (Case 11) while keeping the inflow radial speed constant, the core radius increased consistent with larger S behavior. Also, the maximum tangential speed at the core radius increased because the input angular momentum was doubled, unlike Cases 12 and 13. The inflow angle grew when the tangential speed increased causing an increase in S. When the inflow tangential speed was halved from the control case while keeping the inflow radial speed constant (Case 15), both core radius and S decreased. Maximum tangential speeds decreased since the input angular momentum was halved. Unlike the effect when S was decreased by increasing the inflow radial speed which caused the vortex to be narrow but intense, the reduction of inflow tangential speed made the vortex narrower as well as weaker. Thus, it can be concluded that the core radius is directly proportional to the input S but the vortex intensity depends upon the input angular momentum.

In tests where S was kept constant while doubling both the radial and tangential speeds (Case 16), the core radius stayed the same but the maximum tangential speed almost doubled at 20 m elevation compared with Case 11. When both radial and tangential components of inflow were halved (Case 17) keeping S constant, the core radius was not affected but the peak tangential speed was halved compared with Case 11.

These tests reveal that S determines the core radius of the vortex, agreeing with Doswell and Grazulis, 1998. Because S is a function of the inflow angle (ratio of magnitudes of tangential and radial velocities), the inflow angle in laboratory simulators such as Sarkar, *et al*. (2005) may be the primary mechanism allowing simulation of a wide range of tornado sizes. The maximum tangential speed in the vortex, however, is not a simple function of S. Increases in either radial or tangential inflow (radial momentum flux or inflow angular momentum) can increase the peak tangential flow in the vortex. An increase in the inflow angular momentum resulted in a radial expansion of the core (consistent with a larger S) and intensification of the maximum tangential speed, while an increase in the inflow radial momentum increased the peak tangential speed but reduced the core radius (consistent with a decrease in S). It was also noted that in Cases 13 and 14 (both with relatively high swirl ratios) the radial profile of the tangential speeds broke down at elevations above 420 m with two peaks existing instead of one. Previous studies (Church, *et al*. 1979) concluded that a single laminar vortex was produced with low values of S while a vortex breakdown occurred as S was increased.

The influence of S on radial speed at a given height near the surface (20 m) was also noted. In Case 12, radial flow was always directed inward (negative values) because of the small S of 0.02. In both Cases 11 and 13, the radial speed within the core radius was positive or outward but radial speeds beyond the core radius were negative or inward. Case 11 ($S = 0.09$) had a smaller radius at which the peak positive radial speed occurred and a larger magnitude of this speed compared to Case 13 ($S = 0.44$). Case 15 ($S = 0.02$), having the same small S as Case 12 with halved inflow tangential speeds as Case 11, also had no positive radial speed within the core radius. In the case with an increased inflow tangential speed (Case 14), outward (positive) radial speeds occurred within the core radius as S was increased to 0.36. The stronger inflow tangential speed led to larger peak values of positive radial speed. The three cases, Case 11, 16 and 17, had the same inflow angle or S. All three cases resulted in the same radius for the peak (positive) radial speed, consistent with the same S, while the peak value was larger in Case 16 than in Case 11 due to a stronger

inflow horizontal wind.

It can be concluded from the above tests that there is only inward flow within the vortex when S is small. Larger S results in positive radial speed within the core, and if it occurs, then the radius of the positive peak radial speed will increase as S increases. Past work also showed that when S is large enough, a downdraft will occur in the vortex core (Dowell, *et al*. 2005) and cause outward flow within the core radius region. The radius of the peak positive radial speed was slightly smaller than the core radius. The magnitude of the peak positive speed depends upon the input radial speed or tangential speed, as seen in Cases 13 and 14 which had half the radial speed and doubled tangential speeds compared to Case 11. The peak radial speeds decreased if S increased due to a reduction of inflow radial speed and increased if S increased due to an increase in inflow tangential speed.

For these same inflow sensitivity tests, the impact of changes on turbulent kinetic energy (TKE) was also examined. Within the vortex TKE was extremely large near the surface and decreased with height. A large swirl ratio (Cases 13-14) resulted in a much wider turbulent region than in cases with smaller S which had concentrated regions of TKE near the core that decreased in magnitude as S decreased. Larger TKE values occurred with larger velocities.

5.9. Angular velocity and decay rate

The angular velocity (ω) of the tornado core at a given elevation is defined by $V_t = \omega r$ which gives the linear relationship between the tangential speed (V_t) and radius (r) in the forced vortex region inside the core. The decay rate (n) can be defined as $V_t r^n = C$, where C is a constant, which gives the relationship between V_t and r in the region outside the core. It is equal to 1 for a Rankine vortex, and at the radius of the core $V_t r_c^n = \omega r_c^{n+1} = C$. The angular velocity and the decay rate were estimated at both 20 m and 110 m elevations for all the numerical simulations (Table 3). The angular velocity is usually larger at 20m than at 110m elevation because the tangential speed is larger while the core radius is smaller (giving the tornado a funnel shape). In most cases, the decay rate was slightly smaller than 1.0 and the decay rate at 20m was greater in magnitude than that at

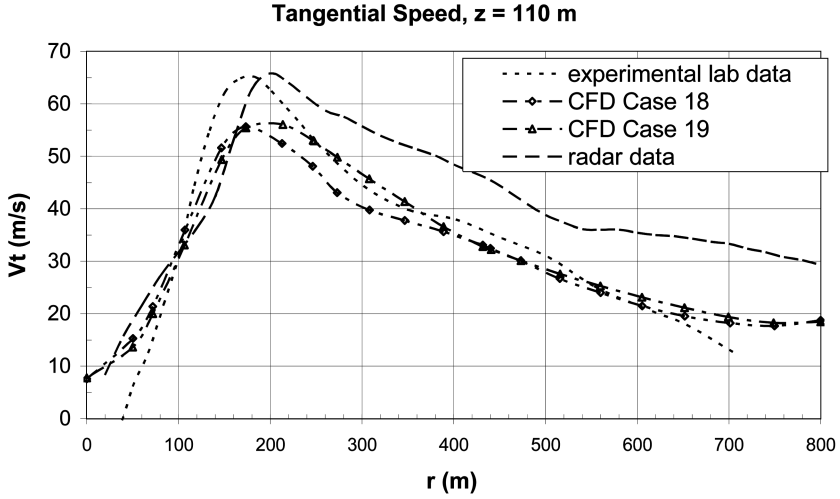

Fig. 5 Comparison of CFD Cases 18 and 19 with measured lab data and radar data

110m. Both these trends are similar to the radar data and the laboratory data. In Cases 11-17, where S was varied, the decay rates did not change, so it can be concluded that the decay rate is independent of S. Surprisingly, the decay rate at the lower elevation, 20m, was less sensitive to changes in roughness than it was at 110m, as seen in a comparison of Cases 9 and 10 with Case 1. The same trend was found comparing Cases 19 and 18.

5.10. Comparison of CFD simulations with radar data

Tangential speeds at 110 m elevation in Case 9 (surface roughness) compared well with Doppler radar measurements in the tornado (Fig. 6a). Good agreement was also evident for the core radius, maximum tangential speed, swirl ratio, angular velocity, and decay rate (Table 3). These data

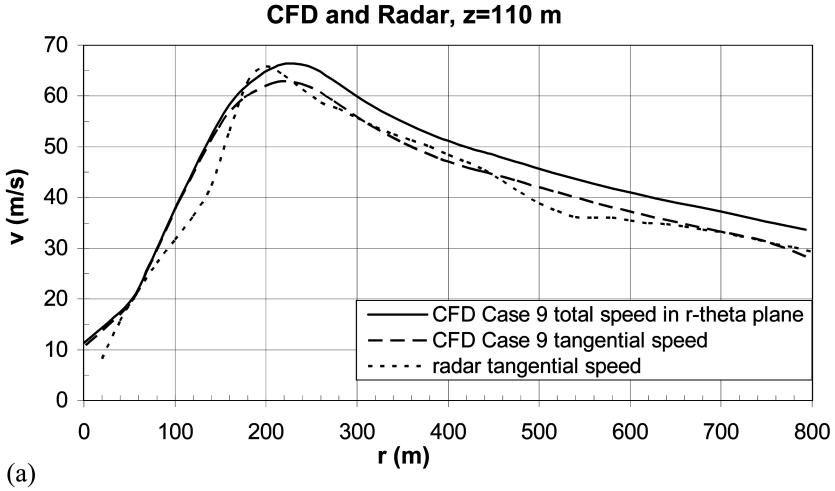

(a)

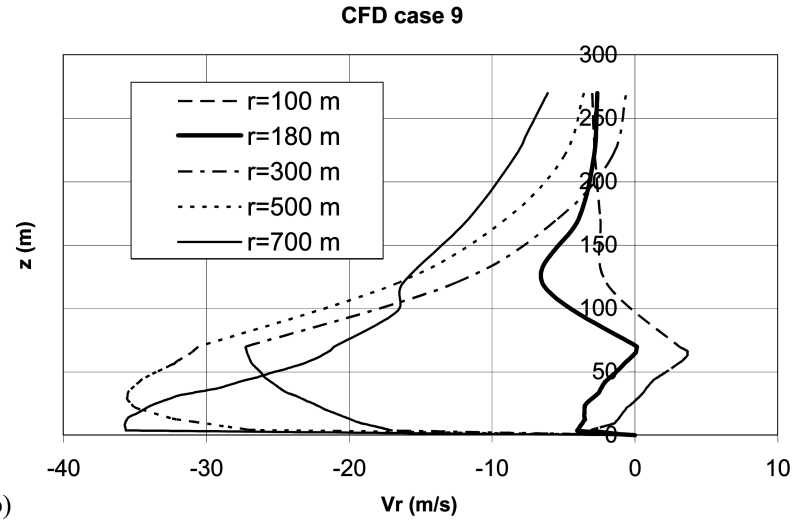

(b)

Fig. 6 (a) Comparison of CFD Case 9 total speed and tangential speed with observed radar tangential speed, (b) CFD Case 9 radial speed

suggest it is possible to simulate the real case using the ISU laboratory tornado simulator if the surface roughness is modeled properly. The total speed on the horizontal plane, of significance to engineering, was found to exceed the tangential speed (Fig. 6a). The magnitude of the radial speed (Fig. 6b) decreases with decreasing radius. The elevation at which the maximum radial speed occurs first increases and then decreases with decreasing radius. Also, the radial speeds within the core, e.g., r = 100m, become alternately positive (outward) and negative (inward) with height, a trend also observed in the radar data (Fig. 3).

6. Summary and conclusions

The sensitivity of computational simulations of a tornado to geometric parameters and surface roughness within a domain based on the ISU laboratory tornado simulator was investigated. The first goal of this study was to verify how well the CFD model, when driven by far field radar observations and laboratory measurements, could capture the flow characteristics of both full scale and laboratory-simulated tornadoes. A second goal was to use the model to examine the sensitivity of the simulations to various parameters that might affect the laboratory simulator tornado. An understanding of these results is important since radar data are not accurate below 20-50 m, and numerical simulation may be needed to estimate near-ground winds.

The mesh size used in the model impacted the simulations, with a larger mesh reducing the magnitude of the tangential speed. An examination of convergence found that a grid with a 5 m mesh at lower elevations (<70 m) and a 50 m mesh above (Table 2, Fig. 4) produced results within 20-30% of converged values, and hence this mesh was deemed acceptable for our sensitivity studies.

These sensitivity tests found that a larger inflow radius created a wider vortex. The radius of the outflow cylinder controlled both the size and intensity of the vortex. Enlarging the outflow radius increased the core radius while reducing the tangential velocities at all levels. Additionally, it was found that beyond a critical ratio of the length of the control domain cylinder (h4) to the diameter of the outflow cylinder (d2) of 1, an increase in the length of the control domain cylinder did not change the maximum tangential speed but did increase the core radius. Below this critical value, a reduction in the length of the control domain cylinder did not change the core radius but increased the maximum tangential speed. Defining of the side wall of the control cylinder to be outflow instead of a rigid wall resulted in better agreement of both the core radius and peak tangential speed with radar data, possibly because the allowable flow structure resembled nature better.

As found in earlier studies (Lewellen, D.C. and Lewellen, W.S. 1997, Dessens 1972, Wilkins, *et al*. 1975) our tests showed that surface roughness influences tornado dynamics. Surface roughness markedly decreased peak tangential speed, which occurs at low levels, but had a reduced impact at higher levels. Surface roughness enlarged the vortex core radius and reduced tangential speed. It also made the flow more turbulent, possibly leading to a more destructive vortex because the speed and directions of the wind would fluctuate rapidly (Leslie 1977).

It was also shown that the numerical model can simulate lab data reasonably well. After roughness was applied to computational model of the laboratory simulator, flow characteristics within its vortex agreed better with radar observations. It thus appears the lab simulator can accurately reproduce real tornado structure if roughness is modeled properly.

Swirl ratio tests founds that the core radius was directly proportional to the swirl ratio of the vortex generated. However, the vortex intensity or magnitude of the maximum tangential speed depends upon the input angular momentum or tangential speed distribution at the far field. The

maximum tangential speed was also sensitive to changes in S for a given input angular momentum. Since the core radius changes with S while the angular momentum at the radius of the core is proportional to the input angular momentum, an increase in swirl ratio increases the core radius and decreases the maximum tangential speed. The swirl ratio influences the nature of the radial speed at a given height close to the ground surface. There is only inward flow within the vortex when S is small. Larger swirl ratios of 0.9 resulted in positive radial speed within the core, and the radius of the positive peak radial speed will increase as S increases. The radius of the peak positive radial speed was slightly smaller than the core radius; the peak positive radial speed itself depends upon the input radial (or tangential) speed.

Within the vortex, TKE was found to be extremely large near the surface, and it decreased with height. A large swirl ratio resulted in a much wider turbulent region than one associated with smaller swirl ratio. Those cases with small S had a concentrated region of TKE near their core that decreased with a further decrease in S.

Both the angular velocity and the decay rate at low elevation (20 m) were larger in magnitude than they were at high elevation (110 m) for all the tests, a result consistent with field observations. It was found that the decay rate is independent of S but influenced by the surface roughness at high elevations.

It was noted that the core radius, maximum tangential speed, swirl ratio, angular velocity and decay rate matched quite well with those of the Doppler radar when surface roughness was introduced.

Further quantification of the sensitivity of the simulated tornado to surface roughness will be the subject of future work. The tornado characteristics observed over different types of terrain will also be studied. These numerical tests are particularly important to help the ISU laboratory simulations better emulate the field characteristics of tornadoes so that loading effects on typical structures can be assessed. Knowledge of these loads may lead to design strategies that can enable some structures to be resistant to tornado winds, reducing the losses caused by tornado events.

Acknowledgements

This research was funded by National Science Foundation Grant 0220006. The authors would like to thank Daryl Herzmann and Jim Wellman for their technical computer support.

References

Alexander, R.C. and Wurman, J.M. (2005), "The 30 May 1998 Spencer, South Dakota, storm. Part I: the structural evolution and environment of the tornadoes", *Mon. Weather Rev.*, AMS, **133**, 72-96.

Bluestein, B.H. and Pazmany, L.A. (2000), "Observations of tornadoes and other convective phenomena with a mobile 3-mm wavelength Doppler radar: The spring 1999 field experiment", *Bull. American Meteorological Society*, **81**, 2939-2951.

Church, C.R., Snow, J.T., Baker, G.L. and Agee, E.M. (1979), "Characteristics of tornado-like vortices as a function of swirl ratio: A laboratory investigation", *J. Atmos. Sci.*, **36**, 1755-1776.

Davies-Jones, P.R. (1973), "The dependence of core radius on swirl ratio in a tornado simulator", *J. Atmos. Sci.*, **30**, 1427-1430.

Dessens, J. (1972), "Influence of ground roughness on tornadoes: A laboratory simulation", *J. Appl. Meteorol.*, **11**, 72-75.

Diamond, C.J. and Wilkins, M.E. (1984), "Translation effects on simulated tornadoes", *J. Atmos. Sci.*, **41**(17),

2574-2580.
Doswell, C.A. and Grazulis, P.T. (1998), "A demonstration of vortex configurations in an inexpensive tornado simulator", *Preprints, 19th Conf. Severe Local Storms*, Minneapolis, MN, American Meteorological Society, 85-88.
Dowell, D.C., Alexander, C.R., Wurman, J.M. and Wicker, J.L. (2005), "Centrifuging of hydrometeor and debris in tornadoes: radar-reflectivity patterns and wind-measurement errors", *Mon. Weather Rev.*, AMS, **133**, 1501-1524.
Fluent, Inc. (2005), *FLUENT 6.2 User's Guide*, Lebanon, NH.
Gallus, Jr., W.A., Sarkar, P.P., Haan, Jr., F.L., Le, K., Kardell, R. and Wurman, J. (2004), "A translating tornado simulator for engineering tests: Comparison of radar, numerical model, and simulator winds", *Preprints, 22nd Conf. Severe Local Storms*, Hyannis, MA, American Meteorological Society.
Gallus, Jr., W.A., Haan, Jr., F.L., Sarkar, P.P., Le, K. and Wurman, J. (2006), "Comparison of numerical model and laboratory simulator tornado wind fields with radar observations of the Spencer, South Dakota tornado", *Symp. on the Challenges of Severe Convective Storms*, 86th AMS Annual Meeting, Atlanta, GA, American Meteorological Society.
Haan, F.L., Sarkar, P.P. and Gallus, W.A. (2008), "Design, construction and performance of a large tornado simulator for wind engineering applications", *Eng. Struct.*, **30**, 1146-1159.
Hu, M., Xue, M., Brewster, K. and Gao, J. (2004), "Prediction of Fort Worth tornadic thunderstorms using 3DVAR and cloud analysis with WSR-88D Level-II data", *Preprints, 22nd Conf. Severe Local Storms*, Hyannis, MA, American Meteorological Society, CDROM, J1.2.
Jischke, M.C. and Light B.D. (1983), "Laboratory simulation of tornadic wind loads on a rectangular model structure", *Proceedings of the Sixth International Conf. on Wind Engineering*, Australia and New Zealand.
Kondo, J. and Yamazawa, H. (1986), "Aerodynamic aerodynamic roughness over an inhomogeneous ground surface", *Bound-Lay. Meteorol.*, **35**, 331-348.
Lettau, H. (1969), "Note on aerodynamic roughness-parameter estimation on the basis of roughness-element description", *J. Appl. Meteorology*, **8**, 828-832.
Leslie, W.F. (1977), "Surface roughness effects on suction vortex formation", *J. Atmos. Sci.*, **34**, 1022-1027.
Lewellen, D.C. and Lewellen, W.S. (1997), "Large eddy simulations of a tornado's interaction with the surface", *J. Atmos. Sci.*, **54**(5), 581-605.
Lewellen, W.S., Lewellen, D.C., Xia, J. (1999), "The influence of a local swirl ratio on tornado intensification near the surface", *J. Atmos. Sci.*, **57**, 527-544.
Lewellen, D.C. and Lewellen, W.S. (2007a), "Near-surface intensification of tornado vortices", *J. Atmos. Sci.*, **64**(7), 2176-2194.
Lewellen, D.C. and Lewellen, W.S. (2007b), "Near-surface vortex intensification through corner flow collapse", *J. Atmos. Sci.*, **64**(7), 2195-2209.
Stull, R.B. (1988), *An Introduction to Boundary Layer Meteorology*, Kluwer Academic Publishers.
Snow, J.T. and Lund, D.E. (1988), "A second generation tornado vortex chamber at Purdue University", *Preprints, 13th Conf. Severe Local Storms*, Tulsa, Oklahoma, American Meteorological Society, 323-326.
Simiu, E. and Scanlan, R. H. (1996), *Wind Effects on Structures: Fundamentals and Applications to Design*, 3rd edition. John Wiley and Sons, New York.
Selvam, R.P. and Millett, P.C. (2003), "Computer modeling of the tornado-structure interaction: investigation of structural loading on cubic building", *Wind Struct.*, **6**(3), 209-220.
Sarkar, P.P., Haan, F.L., Gallus, W.A., Kuai, L., Kardell, R., Wurman, J.M. (2005), "A laboratory tornado simulator: comparison of laboratory, numerical and full-scale measurements", *10th Americas Conference on Wind Engineering*, Baton Rouge, US, American Association for Wind Engineering.
Ward, N.B. (1972), "The exploration of certain features of tornado dynamics using a laboratory model", *J. Atmos. Sci.*, **29**, 1194-1204.
Wilhelmson, R.B. and Wicker, L.J. (2001), "Numerical modeling of severe local storms", *Severe Convective Storms, Meteor. Monogr.*, American Meteorological Society, **28**(50), 123-166.
Wilkins, M.E., Sasaki, Y., Johnson, H.L. (1975), "Surface friction effects on thermal convection in a rotating fluid: A laboratory simulation", *Mon. Weather Rev.*, AMS, **103**, 305-317.
Wurman, J. and Gill, S. (2000), "Finescale radar observations of the Dimmitt, Texas (2 June 1995) tornado",

Mon. Weather Rev., AMS, **128**, 2135-2164.
Wurman, J.M. (2002), "The multiple vortex structure of a tornado", *Weather Forecas.*, **17**, 473-505.
Wurman, J.M. and Alexander, C.R. (2005), "The 30 May 1998 Spencer, South Dakota, storm. Part II: comparison of observed damage and radar-derived winds in the tornadoes", *Mon. Weather Rev.*, AMS, **133**, 97-119.

CC